Scientific African 4 (2019) e00094

Contents lists available at ScienceDirect

Scientific African

journal homepage: www.elsevier.com/locate/sciaf

Modeling the spatial distribution of Global Solar Radiation (GSR) over Ghana using the Ångström-Prescott sunshine duration model

Prince Junior Asilevi[a,b,*], Emmanuel Quansah[b], Leonard Kofitse Amekudzi[b], Thompson Annor[b], Nana Ama Browne Klutse[c]

[a] School of the Environment and Safety Engineering, Jiangsu University, P.R. China
[b] Department of Physics, Kwame Nkrumah University of Science and Technology, Kumasi, Ghana
[c] Department of Physics, University of Ghana, Legon, Accra, Ghana

ARTICLE INFO

Article history:
Received 27 December 2018
Accepted 21 May 2019

Keywords:
Ångström–prescott
Sunshine duration model
Global solar radiation
and Gridding

ABSTRACT

Solar radiation is an important geological and meteorological parameter. In most developing countries, data is readily unavailable owing to lack of instrumentation and skilled personnel. In this study, Global solar radiation (GSR) over Ghana has been quantified using the Ångström–Prescott sunshine model with sunshine duration data from 22 synoptic stations distributed across the country's ecological zones. The simulated data was gridded at 10 km by 10 km, establishing the spatial distribution of solar radiation over the country. Comparison with satellite data showed good results with root mean square error (RMSE) values of 1–5 $MJm^{-2}day^{-1}$ and correlation coefficient of 60 - 66%. Meanwhile, the estimated total GSR over the country was found to be 412.82 $MJm^{-2}day^{-1}$. The savanna zone had the maximum estimated total monthly mean GSR for the year, with the highest value of 20.76 $MJm^{-2}day^{-1}$ in Navrongo. The forest zone had the minimum estimated total annual mean GSR, with the lowest radiation level in Oda (17.11 $MJm^{-2}day^{-1}$). A maximum and minimum mean clearness index of 0.59 and 0.48 respectively are estimated, implying that about 53% of solar radiation at the top of the atmosphere reaches the study area after attenuation. The satellite data has a total monthly mean horizontal Global Solar irradiance of 366.62 $MJm^{-2}day^{-1}$. The study shows that the region is a potential field to harness and optimize solar energy for the operation of photovoltaic systems and solar collectors for industrial and domestic applications.

© 2019 The Authors. Published by Elsevier B.V. on behalf of African Institute of Mathematical Sciences / Next Einstein Initiative.
This is an open access article under the CC BY license.
(http://creativecommons.org/licenses/by/4.0/)

1. Introduction

Energy from the sun reaching the earth in the form of electromagnetic radiation is the driver of almost all physical processes on earth. This energy is readily available to provide electricity and heat for both industrial and domestic applications [1, 2].

* Corresponding author.
E-mail address: 5103171307@stmail.ujs.edu.cn (P.J. Asilevi).

https://doi.org/10.1016/j.sciaf.2019.e00094
2468-2276/© 2019 The Authors. Published by Elsevier B.V. on behalf of African Institute of Mathematical Sciences / Next Einstein Initiative. This is an open access article under the CC BY license. (http://creativecommons.org/licenses/by/4.0/)

The use of non-renewable sources of energy such as coal, gasoline, and other forms of fossil fuels have been identified as contributing significantly to net greenhouse gas emission thereby increasing global mean temperature. It has therefore become necessary to explore energy from renewable sources. In addition, increasing demand for energy has been identified as the mark of a growing economy. Unfortunately, this demand has not been satisfactorily addressed. These and many other concerns have promoted the edge to probe the production of energy for industrial and domestic use from environmentally clean and renewable sources of energy, such as solar and wind. This has been the effort of the Solar and Wind Energy Resource Assessment (SWERA) under the United Nations Environment Program (UNEP) [3, 4].

A major challenge facing solar energy technology is the availability of solar radiation data at the area of interest, especially for developing countries to enhance a realistic solar energy potential. This has been attributed to the cost of measurement instruments. It has been demonstrated that, the solution to the lack of data will be to estimate solar radiation from readily available meteorological data such as ambient temperature, precipitation, relative humidity, sunshine duration, and altitude [5–7].

Empirical models for estimating GSR from sunshine duration have been reportedly used all around the world, and for selected sites in Ghana [8, 9]. Forson et al. [10] reported appreciable statistical performance when the Ångström – Prescott sunshine based empirical model prediction is compared with measured data for Kumasi. Sarsah and Uba [11] in a similar analysis, validated solar radiation estimates with ground measured data at Wa Polytechnic. However, a nationwide estimation is lacking.

In this study, the Angstrom – Prescott sunshine based empirical model is employed to predict and analyze the solar radiation pattern over Ghana, using sunshine duration data for twenty two synoptic stations across the country, obtained from the Ghana Meteorological Agency (GMet). The predicted dataset is then gridded at a spatial resolution of 10 km by 10 km, establishing the distribution of solar radiation across the ecological zones of the country, and then compared with Meteosat data obtained from the German Aerospace Centre (DLR).

2. Materials and methods

2.1. Study area

According to the Ghana Meteorological Agency (GMet) classification, the country is grouped into four agro-ecological zones. From the north to south, the agro-ecological zones are the Savannah, Transition, Forest, and Coastal zones [12].

The climate of the country is a tropical monsoon or the West African Monsoon (WAM), with two main seasons namely the wet and dry seasons. This climate of the region is modulated by the oscillation of the Inter-Tropical Discontinuity (ITD), the gradient created by the convergence of moisture laden air mass from the Gulf of Guinea and the dry northeast continental tropical air mass. The forward and backward motion of the ITD across the region results is a two rainfall regime: bi-modal in the south (coastal and forest zones) and uni-modal in the northern half of the country (part of the transition and savannah zones) [13, 14].

2.2. Data and method

Sunshine duration data from twenty two Ghana Meteorological Agency (GMet) synoptic stations distributed across the country, and GSR Meteosat-7 satellite data from the Solar and Wind Energy Resource Assessment (SWERA) project, under the United Nations Environment Program (UNEP) covering the period of 2000 to 2002 were used. The sunshine duration data was measured with the Campbell-Stokes sunshine recorder, while the satellite data was prepared by the German Aerospace Centre (DLR) for the SWERA operations at a resolution of 10 km by 10 km [14, 4]. Fig. 1 shows the position of the stations across the country.

The modified Angstrom – Prescott sunshine model used in the study, is given by Eq. (1).

$$\mathbf{H} = \left(0.25 + 0.5\frac{\mathbf{n}}{\mathbf{N}}\right)\left[\frac{24 \times 60}{\pi}\mathbf{G_{sc}}\mathbf{d_r}\left(\boldsymbol{\omega_s}\sin\boldsymbol{\varphi}\sin\boldsymbol{\delta} + \cos\boldsymbol{\varphi}\cos\boldsymbol{\delta}\sin\boldsymbol{\omega_s}\right)\right] \tag{1}$$

where H ($\mathbf{MJm^{-2}day^{-1}}$) is the monthly mean GSR at the ground, $\mathbf{G_{sc}}$ is the solar constant approximately 1365 W$\mathbf{m}^{-2}$, d_r is the relative Earth-Sun distance, n is the measured monthly mean sunshine duration, and N is the full length of the day in hours (day length). The length of each day within the year is given by:

$$\mathbf{N} = \frac{2}{15}\cos^{-1}\left(-\tan\phi\tan\boldsymbol{\delta}\right) \tag{2}$$

$\boldsymbol{\omega_s}$ is the sunset hour angle given by:

$$\boldsymbol{\omega_s} = \cos^{-1}\left(-\tan\phi\tan\boldsymbol{\delta}\right) \tag{3}$$

Where ϕ is the latitude of the point station on the earth surface in degrees, and $\boldsymbol{\delta}$ is the declination angle of the earth in degrees. The angle of declination for a particular Julian day is computed from [7]:

$$\boldsymbol{\delta} = 23.45\sin\left(\frac{102240 + [360 \times \mathbf{J}]}{365}\right) \tag{4}$$

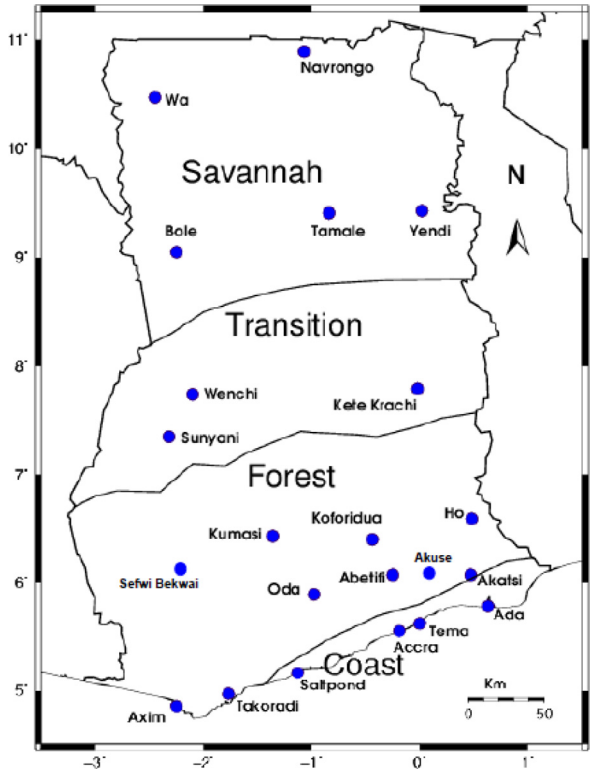

Fig. 1. Map of Ghana, showing all twenty-two sites of the Ghana Meteorological Agency (GMET) Synoptic stations recording sunshine duration. Adapted from Amekudzi et al. [12].

Where J represents the number for the Julian day of the year (first January is 1 and second January is 2). The clearness index (K_T) which is the ratio of the amount of solar radiation at the ground (H) to the extraterrestrial solar radiation (H_O) is given by:

$$K_T = H/H_O \tag{5}$$

The clearness index is a good indicator of the degree of opacity of the atmosphere, due to factors such as clouds, water vapour and aerosol, hence the fraction of extraterrestrial solar radiation reaching the ground [16].

The ratio n/N is called the cloudless index. It describes how much clouds exist for a particular day, hence classifying the atmosphere over of the study area as clear sky, cloudy, or overcast [17]. In this study the values of a (0.25) and b (0.5) from [18], which were calculated from experimental data, were used. Eq. (5) is an index of the transmittance of the overlaying sky and hence a measure of the amount of radiation reaching the study area. According to Carvalho [19], a clearness index of 0 – 3.0 characterizes a cloudy sky while a clearness index of 0.65 – 1.0 characterizes a clear sky.

The Minimum Surface Curvature (MSC) gridding and its Computational implementation is described in [20]. According to this gridding technique, the interpolated surface generated by the Minimum curvature method is analogous to a thin, linearly elastic plate passing through each of the data values with a minimum amount of bending. The algorithm of the MSC method is based on the numerical solution of the modified bi-harmonic differential equation:

$$\nabla^4 = \frac{\partial^4 \mathbf{f}}{\partial \mathbf{x}^4} + \frac{\partial^4 \mathbf{f}}{\partial \mathbf{y}^4} + \frac{2\partial^4 \mathbf{f}}{\partial \mathbf{x}^2 \partial \mathbf{y}^2} \tag{6}$$

If the tensioning parameter $T = 0$, the bi-harmonic differential equation is solved; if $T = 1$, the Laplace differential equation is solved; in this case the resulting surface may have local extremes only at points XYZ. Smith and Wessel [20] have demonstrated that, the minimum surface curvature method of gridding is a universal method suitable for smooth approximation and interpolation.

The Root Mean square Error (RMSE) and Mean Percentage Error (MPE) were used to test for agreement between the estimated dataset and the DLR satellite data. According to Khalil [21] and Quansah [7], RMSE and MPE are given in Eqs. (7) and 8:

$$\mathbf{RMSE} = \sqrt{\frac{1}{\mathbf{x}} \sum_{\mathbf{i}=1}^{\mathbf{x}} (\mathbf{G_{cal}} - \mathbf{G_{sat}})^2} \tag{7}$$

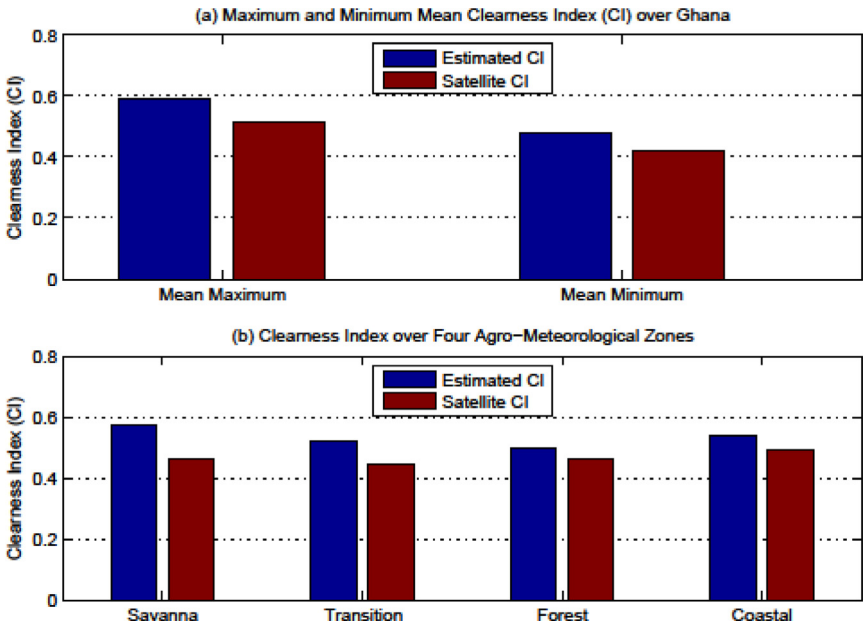

Fig. 2. Clearness Index (CI) over Ghana: (a) monthly mean maximum and minimum CI over the country and (b) Clearness Index (CI) for all the four agro-ecological zones.

$$\mathbf{MPE} = \frac{1}{\mathbf{x}} \sum_{\mathbf{i}=1}^{\mathbf{x}} \left(\frac{\mathbf{G_{sat}} - \mathbf{G_{cal}}}{\mathbf{G_{sat}}} \times 100 \right) \tag{8}$$

Where $\mathbf{G_{cal}}$ and $\mathbf{G_{sat}}$ are the estimated and satellite values respectively ($\mathbf{MJm^{-2}day^{-1}}$), for x number of observations. From Khalil and Shaffie [21], very good RMSE values are closer to zero, with zero as the best. The MPE is also an indicator of the percentage deviation of the estimated dataset for measured radiation dataset [7].

3. Results and discussion

3.1. Clearness index over Ghana

The transparency (Clearness Index) of the overlaying atmosphere is a crucial determinant for the amount of solar radiation reaching the country [22]. Fig. 2 shows the clearness index over Ghana for both calculated and satellite datasets.

From Fig. 2(b), the clearness index has an estimated value greater than 50% for all the four agro-Meteorological zones. The monthly average maximum and minimum estimated clearness index for the study area is 59% and 47.8%. This indicates a moderately transparent sky across the country. The Forest zone however, shows the lowest clearness index value of 54%. This is attributed to significant cloud cover activities over the region, affording a greater effect of attenuation to solar radiation [13, 15]. The low rainfall regime over the Savanna ecological zone, owing to low relative humidity hence low cloud cover, reflect the high levels of solar radiation over the zone (see Fig. 2).

The implication of having mean clearness index greater than fifty percent is that the sky is moderately transparent throughout the study area, and indicates that solar energy can be efficiently harnessed for technology such as solar farms. The satellite clearness index is relatively lower compared with the estimated clearness index. This could be attributed to the simplicity of the AP model employed in this study, as reported by Poudyal [15] for the Trans-Himalayan region in Nepal, a member country of the SWERA project [23].

3.2. Monthly trend of global solar radiation over the agro ecological zones

A mean daily GSR of 20.22 $\mathbf{MJm^{-2}day^{-1}}$ is estimated for the savanna zone (see Fig. 3a), with Navrongo having the highest insolation (22.57$\mathbf{MJm^{-2}day^{-1}}$). The zone experiences the highest insolation during the dry periods of the year for a sustained four month period (February to May), and then suffers a decline.

Apparently, the lowest insolation levels were estimated for the wet period of the zone from June to September. August is exclusively the month with the lowest estimated insolation. The significantly reduced insolation levels at this time of the annual period, coincides with the period of heavy rainfall season for the zone. The atmosphere at this time of the year is

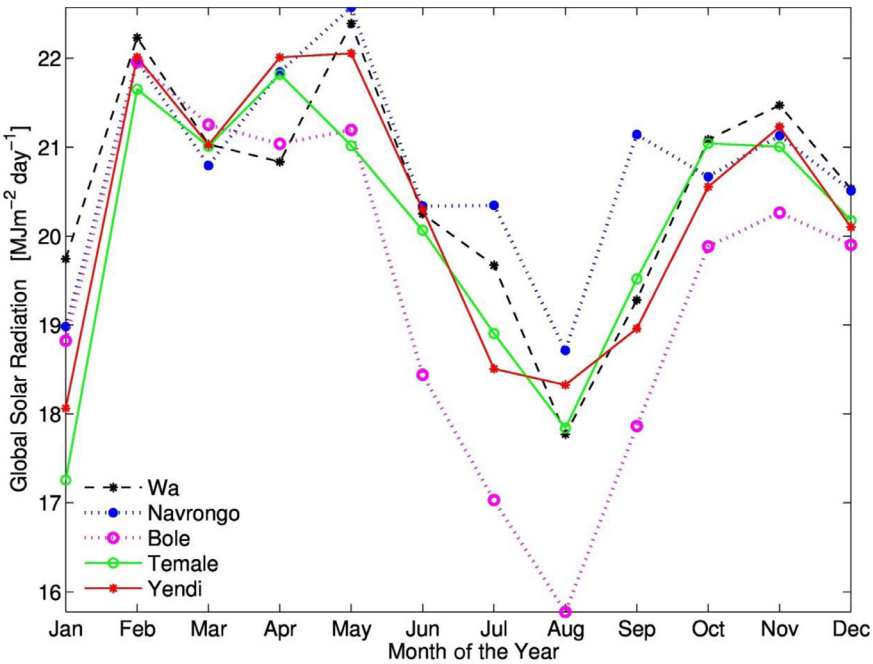

Fig. 3. Monthly mean variation of Global Solar Radiation (GSR) for the Savanna zone.

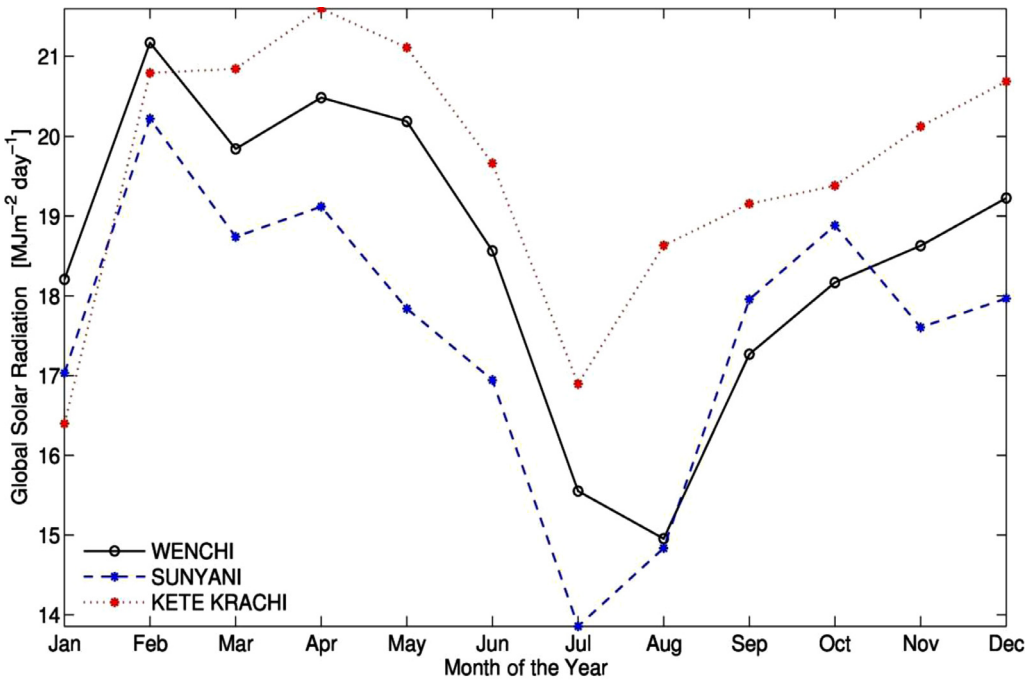

Fig. 4. Monthly mean variation of Global Solar Radiation (GSR) for the Transition zone.

largely moist-laden, with an abundance of precipitation clouds and an overall increase in convective activities preventing solar radiation from reaching the ground.

In the transition zone (see Fig. 4), GSR increases at the commencement of the annual period from January to a maximum in February. This maximum insolation is shortly sustained for a three month period (February to April) and then suffers a sharp decline in May. The model estimated a relatively lower daily mean horizontal Global solar irradiance of 18.57 $\mathbf{MJm^{-2}day^{-1}}$, compared with the savanna zone. In this zone as with the savanna, the lowest GSR was estimated for the wet periods of the year, between July and August. With a monthly mean clearness index of 57% and an annual mean

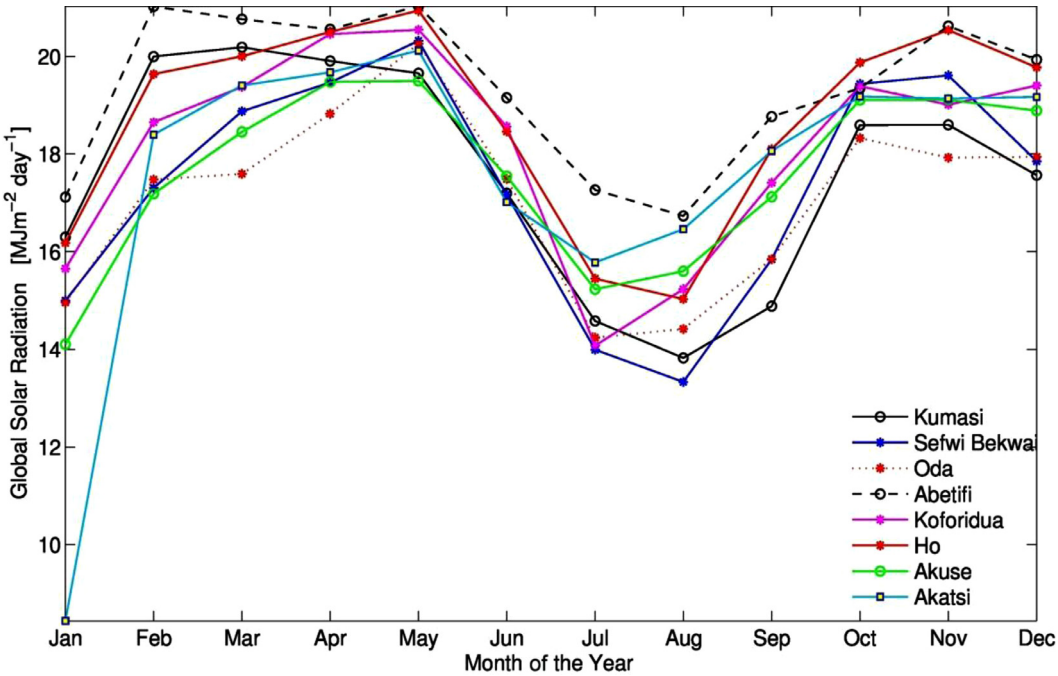

Fig. 5. Monthly mean variation of Global Solar Radiation (GSR) for the Forest zone.

GSR range between 21.6 **MJm**$^{-2}$**day**$^{-1}$ and 15.8 **MJm**$^{-2}$**day**$^{-1}$, the zone recieves good amount of solar radiation within an annual period.

The Forest zone (see Fig. 5) displays for its monthly pattern two distinct periods of maximum GSR: a longer period of maximum solar insolation (between 19.5 **MJm**$^{-2}$**day**$^{-1}$ and 21.0 **MJm**$^{-2}$**day**$^{-1}$) dominates the zone in the first half of the year (February - May) and a very short period of relatively lesser insolation (between 17.9 **MJm**$^{-2}$**day**$^{-1}$ and 20.5 **MJm**$^{-2}$**day**$^{-1}$) within the last half of the year (October/November). The two periods of maximum insolation are separated distinctly by a depression of minimum insolation (8.44 **MJm**$^{-2}$**day**$^{-1}$). This minimum insolation period perfectly coincides with the little dry period between the major and minor rainy seasons in the southern part of Ghana. The low insolation is attributed to stratified clouds that barely provide rains, but serve to shield the surface from the Sun's radiation.

In the Coastal zone (see Fig. 6), the model estimated a relatively higher insolation range (between 12.4 **MJm**$^{-2}$**day**$^{-1}$ and 21.8 **MJm**$^{-2}$**day**$^{-1}$) compared with the Forest zone. A maximum longer period of solar insolation (between 20.3 **MJm**$^{-2}$**day**$^{-1}$ and 21.79 **MJm**$^{-2}$**day**$^{-1}$) dominate the zone in the first half of the year (February - May), and a shorter period of relatively maximum insolation (between 18.5 **MJm**$^{-2}$**day**$^{-1}$ and 21.3 **MJm**$^{-2}$**day**$^{-1}$) within the last half of the year (October-November). The lowest insolation is estimated for the major rainfall period, with estimates between 12.4 **MJm**$^{-2}$**day**$^{-1}$ and 15.4 **MJm**$^{-2}$**day**$^{-1}$. The zone comparatively receives more radiation with an appreciable clearness index (0.54) greater than the Forest zone (0.50). This is attributed to the relatively observed lower precipitations over the Coastal zone stipulated by [14].

3.3. Gridded global solar radiation estimate

In January (Fig. 7(i)), the radiation levels over the country is relatively low with monthly average GSR of 16.14 **MJm**$^{-2}$**day**$^{-1}$. This could be attributed to the fact that January falls within the peak period of the Harmattan season during which large amounts of dust exists in the atmosphere [24].

Tserenpurev et al. [25] and Mikami et al. [26] have shown that solar radiation decreases in dusty days due to the scattering and absorption by dust aerosols. This is the case for the country in January. A phenomenal increase in aerosol scattering and absorption decreases sunshine intensity and hence the amount of ground insolation. This is further demonstrated by the fact that, the harmattan season is characterized by a very cold and dry (9 °C) wind, due to decreased short-wave solar radiation absorption at the ground [27].

February (Fig. 7(ii)) is largely the closing period for the harmattan season. During the period, the denser dust particles have settled to the ground and water bodies, leaving only the finer once mostly over the south. The effect of attenuation has significantly reduced over the country, with the ITD still to migrate from the coast. During this period, average solar radiation levels across the country will begin to increase further. This is clearly the case as shown in section 4.2.

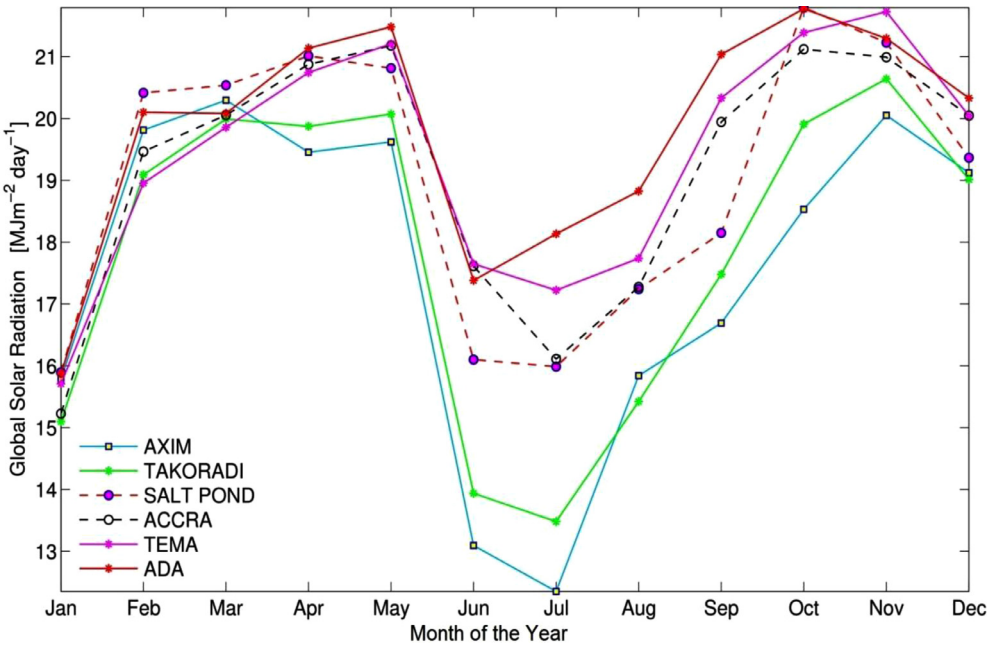

Fig. 6. Monthly mean variation of Global Solar Radiation (GSR) for the coastal zone.

In March (Fig. 7(iii)), the atmosphere is relatively clearer with significantly reduced aerosol concentration. The clearness index over the country reaches 55% for this period. The country receives increasing levels of solar radiation, especially for the savanna zone. At this time the Convergence zone is gradually migrating inland and the atmosphere is becoming clean and moist.

April (Fig. 7(iv)) is also a month with a cleaner and more transparent atmosphere. There is a nation-wide horizontal irradiance with some degree of atmospheric opacity in a few areas of the Forest belt. In general February, March, April and May, are the peak solar radiation periods across the study area.

May (Fig. 7(v)) continues with the longer annual first half maximum horizontal irradiance periods (February to May). A monthly mean Clearness index of 56% is estimated for the month. The west coast in the Transition zone still offers some attenuation. By June (Fig. 7(vi)) the ITD is well migrated into the country. The southern regions experience much convective activities. The atmosphere over the south is very moist laden, once again increasing attenuation by water vapour.

In July (Fig. 7(vii)) the lowest mean clearness index of 45% is estimated over the country. These are very heavy rain periods for most parts of the country, and consequentially very cloudy atmospheres over the sub region. July (Fig. 7(vii)) and August (Fig. 7(viii)) record rains over the entire nation, rendering the atmosphere wet and moist-laden throughout. There is increased attenuation of solar radiation, due mostly to water vapour.

In September (Fig. 7(ix)) the atmosphere is relatively clearer for the north than the much moist-laden south. The atmosphere is still very moist over the Forest and Coastal zones, with estimated solar radiation of 17 $\mathbf{MJm^{-2}day^{-1}}$ and 18.9 $\mathbf{MJm^{-2}day^{-1}}$ respectively.

In October (Fig. 7(x)) when the rains have almost diminished, a transparent nationwide atmosphere is restored. The lesser rains over the savanna zone make it possible for increasing solar radiation.

Though November (Fig. 7(xi)) and December (Fig. 7(xii)) mark the commencement of the harmattan season, the very denser dust particles are yet to take over the entire nation. The phenomenon is gradual, and finds its peak in January when the atmosphere of the entire country densely laden with dust, with very pronounced aerosol scattering and absorption.

October and November afford the country with relatively short but highly transparent atmosphere (with clearness index reaching 60% in November). The country receives very well insolation levels though for a short period just prior to the peak of the harmattan.

The estimated datasets show a downward trend of GSR from October to December (October = 21.8 $\mathbf{MJm^{-2}day^{-1}}$, November = 21.5 $\mathbf{MJm^{-2}day^{-1}}$, and December = 20.5 $\mathbf{MJm^{-2}day^{-1}}$)

3.4. Annual horizontal insolation

Fig. 8 illustrates the estimated annual mean GSR over the four agro-ecological zones of Ghana. It is observed that the country is very well irradiated with the northern half (Savanna and Transition zones) receiving the highest amount of Global solar radiation (22.57 $\mathbf{MJm^{-2}day^{-1}}$), and the southern half, typically the forest zone, receiving the lowest levels of insolation (8.44 $\mathbf{MJm^{-2}day^{-1}}$). This is attributed to low clearness indices. The atmosphere over the zone is highly moist-laden and

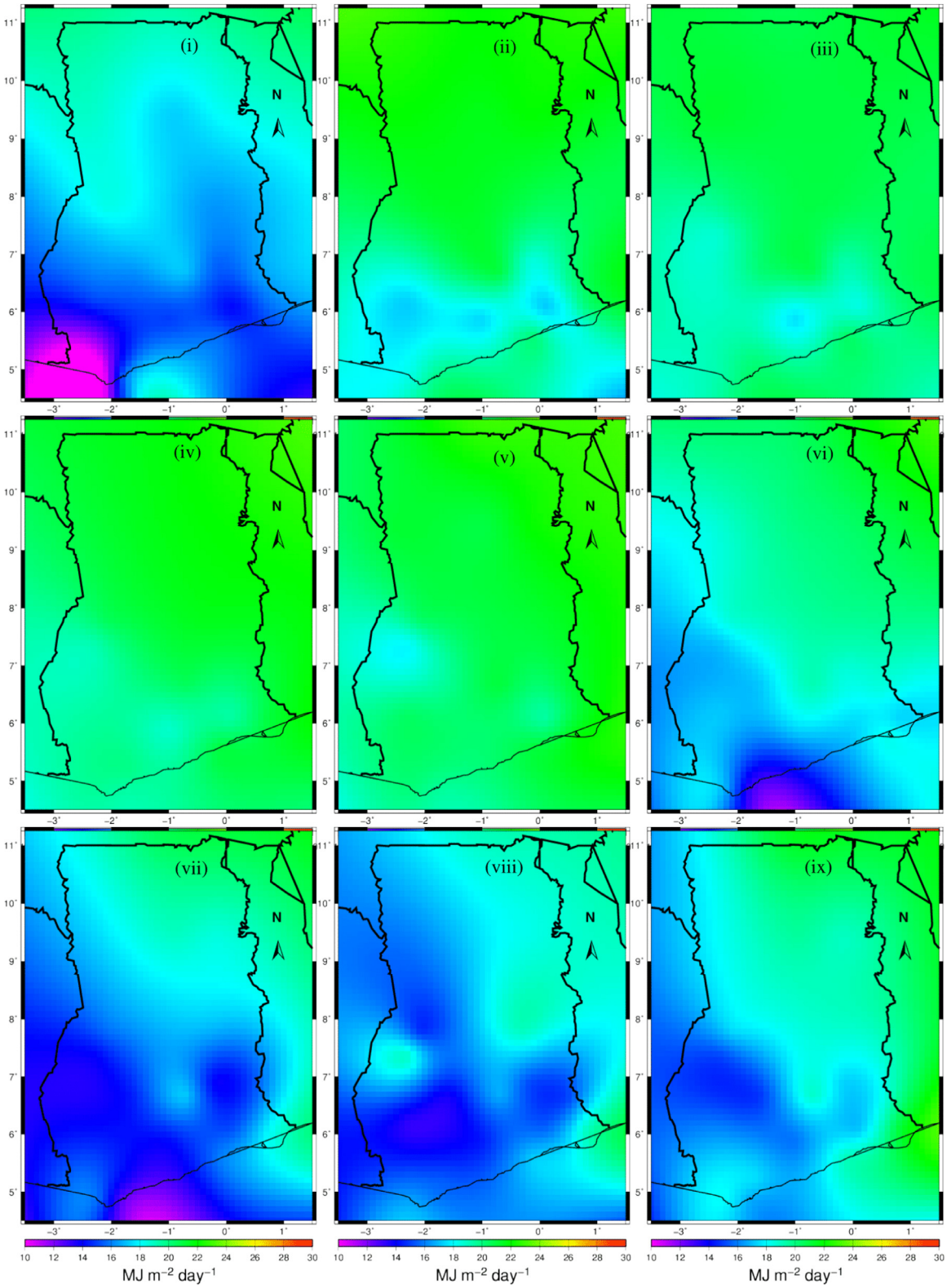

Fig. 7. Gridded Monthly Mean Global Solar Radiation. (i) January, (ii) February, (iii) March, (iv) April, (v) May, (vi) June, (vii) July, (viii) August, (ix) September, (x) October, (xi) November, and (xii) December.

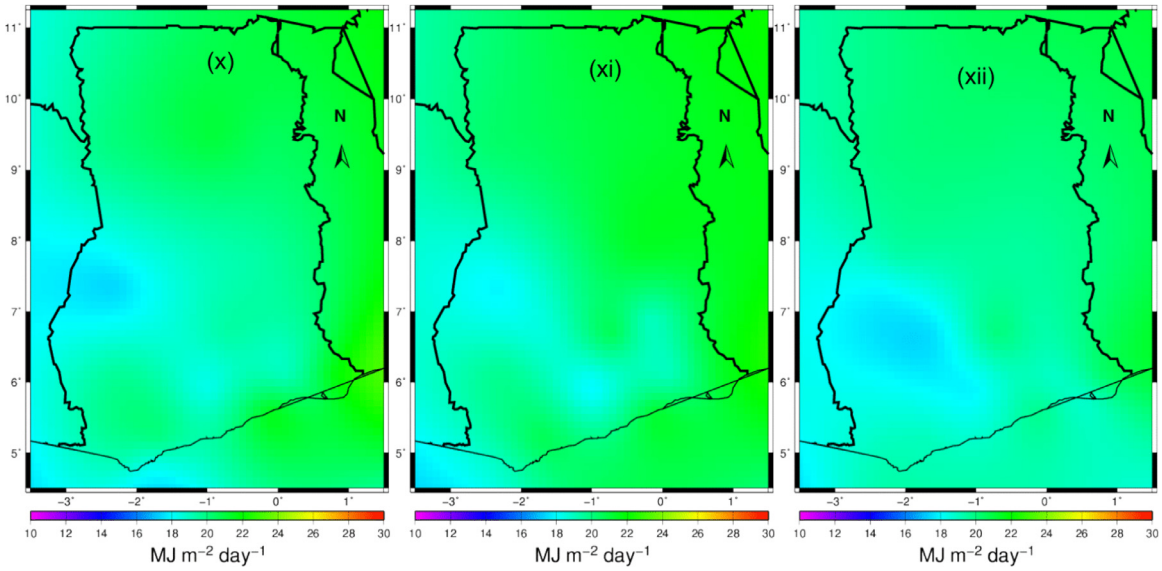

Fig. 7. Continued

Table 1
Estimated seasonal and annual monthly mean GSR. Dec-Jan-Feb (DJF), Mar-Apr-May (MAY), Jun-Jul-Aug (JJA), Sep-Oct-Nov (SON).

Months	Savana	Transition	Forest	Coastal
DJF	20.26	18.95	17.41	18.16
MAY	21.46	19.97	19.23	19.49
JJA	18.82	17.16	15.99	16.27
SON	20.34	18.2	18.49	20.13
Annual	20.22	18.57	17.93	18.76

cloudy, with much convective activities. This is further supported by the fact that the Forest zone records the highest amount of annual mean rainfall.

Table 1 summarizes the estimated seasonal and annual mean Global Solar radiation for the four agro-ecological zones. Each column represents a monthly mean GSR for the particular zone. The savanna zone and the Forest zone are exclusively the regions with the highest and lowest solar radiation levels respectively. For all the zones, the highest solar radiation levels occur in the second trimester (MAM). The third trimester (JJA) is the period with the lowest solar radiation estimates all over the country. This is attributed to the fact that this particular trimester (JJA) is the main rain season for the country, making the atmosphere heavily laden with clouds and water vapour, hence increased absorption of solar radiation.

Annually, the savanna and the transition zones experience the highest irradiation levels, with the southern belt, chiefly the forest zone experiencing the lowest irradiation levels.

The Satellite Global solar radiation datasets were obtained at a 10 km by 10 km spatial resolution. The model estimated datasets have thus been gridded for a 10 km 10 km spatial resolution to enable a statistical performance assessment of the model.

The various statistical tests conducted, showed good agreement between the estimated grids and satellite grid. Fig. 9 shows a comparison between the estimated and satellite grids for September and October. Very few departures were shown between the grids of the two datasets. The sunshine model often had slightly greater estimated solar radiation. This is attributed to the simplicity of the A-P model.

Appreciable root mean square error (RMSE) values between 1 and 5 $MJm^{-2}day^{-1}$ were obtained. This strong statistical correlation is further confirmed by low absolute mean percent error (3 – 29). Also, appreciably positive correlation values between 58% and 70% were obtained.

Conclusions

In this study, the monthly mean Global Solar Radiation (GSR) over Ghana has been estimated using sunshine duration data covering the period of 2000 to 2002 measured at twenty two synoptic stations distributed across the country, using the Ångström – Prescott (AP) sunshine duration model. The estimated monthly mean GSR was gridded at a spatial resolution

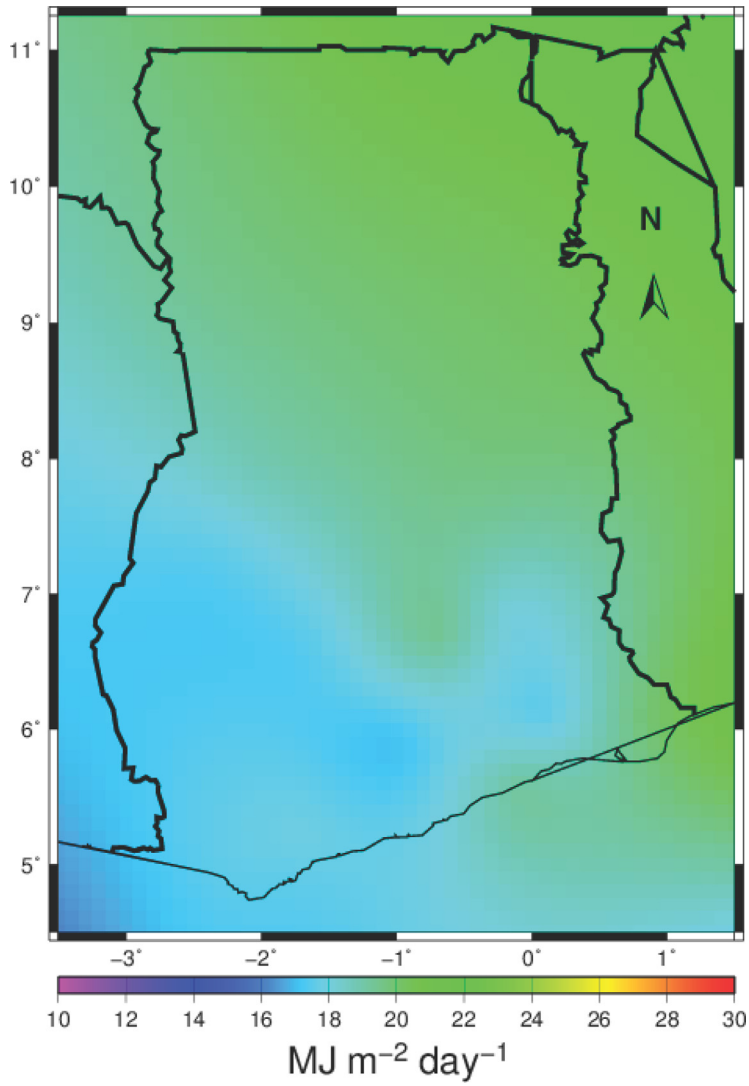

Fig. 8. Annual spatial distribution of monthly mean Global Solar Radiation for year 2000.

(10 km by 10 km), establishing the trend and distribution across the country. Following, the estimated dataset was compared with available satellite data from the German Aerospace Centre (DLR). Statistical tests show good agreement, with appreciable RMSE values between 1 – 5 $MJm^{-2}day^{-1}$ and low absolute mean percent error (3 – 29). The results show that the estimated total monthly mean GSR over the country is 412.82 $\mathbf{MJm^{-2}day^{-1}}$, with the highest solar radiation estimated for the savanna zone at Navrongo (20.76 $\mathbf{MJm^{-2}day^{-1}}$) and the lowest for the forest zone at Oda (17.11 $\mathbf{MJm^{-2}day^{-1}}$). A maximum and minimum monthly mean clearness index of 0.59 and 0.48 respectively are estimated. This means an estimated 53% of solar radiation at the top of the atmosphere reaches the surface of the study area after attenuation. These results agree favorably with the Global solar energy budget presented by Wild [27]. The satellite data has a total monthly mean GSR of 366.62 $\mathbf{MJm^{-2}day^{-1}}$.

The study shows that solar radiation levels over the country (17.11 $\mathbf{MJm^{-2}day^{-1}}$ to 20.76 $\mathbf{MJm^{-2}day^{-1}}$), can afford sufficient energy for solar technology such as photovoltaic systems and solar collectors for industrial and domestic applications. These results may have useful applications in the field of solar energy technology, with regards to the growing demand for energy in the country, and also to better understand the climate system over Ghana.

Conflict of interests

The authors declare that there is no conflict of interests regarding the publication of this paper.

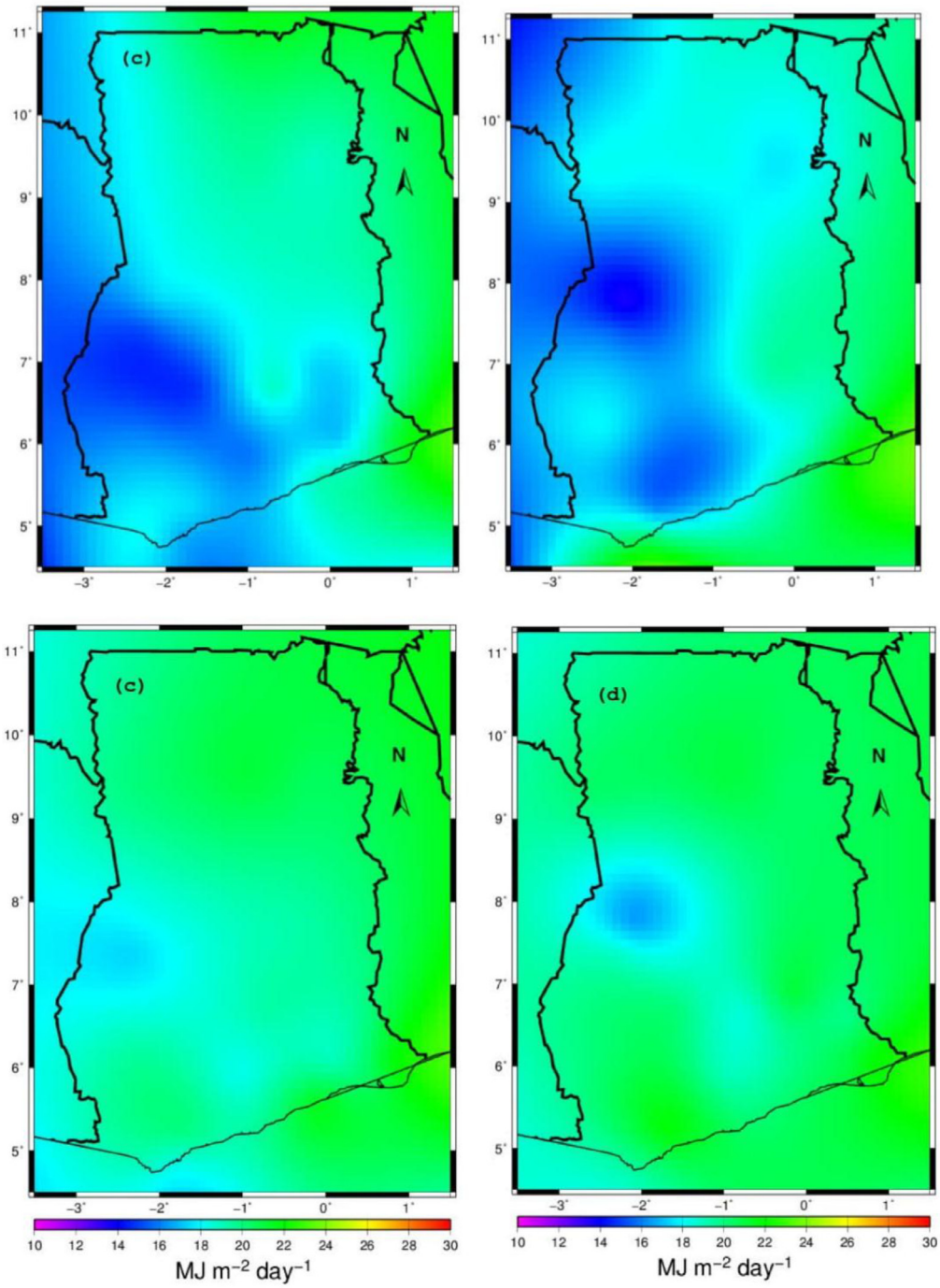

Fig. 9. Gridded horizontal Monthly Mean Global Solar Irradiance: (a) Estimated GSR for September, (b) Satellite GSR for September (c) Estimated GSR for October and (d) Satellite GSR for October.

Acknowledgements

We are thankful to the Ghana Meteorological Agency (GMet) and the Solar and Wind Energy Resource Assessment (SWERA) project, under the United Nations Environment Program (UNEP) for the provision of measured data.

Supplementary materials

Supplementary material associated with this article can be found, in the online version, at doi:10.1016/j.sciaf.2019.e00094.

References

[1] J. Yeaman, A study relating Solar Radiation, Road Surface Temperature and Temperature at Depth in HOT MIX Asphalt, in: Proceedings of the 5th International Conference on Geotechnique, Construction Materials and Environment, 5, GEOMATE International Society, 2015, pp. 536–540.
[2] M.A. El-Shirbeny, B. Abdellatif, Reference Evapotranspiration Borders Maps of Egypt Based on Kriging Spatial Statistics Method, Int. J. Geomate 13 (2017) 1–8.
[3] J. Page, The estimation of monthly mean values of daily total short wave radiation on vertical and inclined surfaces from sunshine records 40s-40n, in: Proc. of UN new sources of energy (Conference paper), 4, Rome, 1967, pp. 378–390.
[4] C. Schillings, R. Meyer, F. Trieb, Solar and wind energy resource assessment (swera), High Resolution Solar Radiation Assessment for Kenya. Final country report prepared by DLR–submitted to UNEP/GEF, 2004.
[5] Y. Charabi, A. Gastli, S. Al-Yahyai, Production of solar radiation bankable datasets from high-resolution solar irradiance derived with dynamical down-scaling numerical weather prediction model, Energy Reports 2 (2016) 67–73.
[6] J.S. Bojanowski, A. Vrieling, A.K. Skidmore, Calibration of solar radiation models for Europe using Meteosat second generation and weather station data, Agricultural Forest Meteorol. 176 (2013) 1–9.
[7] E. Quansah, L.K. Amekudzi, K. Preko, J. Aryee, O.R. Boakye, D. Boli, M.R. Salifu, Empirical models for estimating global solar radiation over the Ashanti region of Ghana, J. Solar Energy 2014 (2014).
[8] K. Anane-Fenin, Estimating solar radiation in Ghana, tech. rep., International Centre for Theoretical Physics, 1986.
[9] C.K. Pandey, A. Katiyar, Solar radiation: models and measurement techniques, J. Energy 2013 (2013).
[10] F. Forson, K. Agbeko, I. Edwin, A. Sunnu, A. Brew-Hammond, F. Akuffo, Solar energy resource assessment for Ghana, Department of Mechanica l Engineering, Kwame Nkrumah University of Science and Technology, 2004.
[11] E.A. Sarsah, F.A. Uba, Monthly-specific daily global solar radiation estimates based on sunshine hours in Wa,Ghana, Int. J. Sci. Technol. Res. 2 (2013) 246–254.
[12] L.K. Amekudzi, E.I. Yamba, K. Preko, E.O. Asare, J. Aryee, M. Baidu, S.N. Codjoe, Variabilities in rainfall onset, cessation and length of rainy season for the various agro-ecological zones of Ghana, Climate 3 (2) (2015) 416–434.
[13] F. Nkrumah, N.A.B. Klutse, D.C. Adukpo, K. Owusu, K.A. Quagraine, A. Owusu, W. Gutowski Jr, et al., Rainfall variability over ghana: model versus rain gauge observation, Int. J. Geosci. 5 (07) (2014) 673.
[14] K. Owusu, P. Waylen, Trends in spatio-temporal variability in annual rainfall in Ghana (1951-2000), Weather 64 (5) (2009) 115–120.
[15] K. Poudyal, B.K. Bhattarai, B. Sapkota, K. Berit, Estimation of global solar radiation using sunshine duration in himalaya region, Res. J. Chem. Sci. 2 (11) (2012) 20–25.
[16] L. Diabate, P. Blanc, L. Wald, Solar radiation climate in Africa, Solar Energy 76 (6) (2004) 733–744.
[17] R. Srivastava, H. Pandey, Estimating angstrom-prescott coefficients for india and developing a corre-lation between sunshine hours and global solar radiation for india, ISRN Renewable Energy 2013 (2013).
[18] R.G. Allen, L.S. Pereira, D. Raes, M. Smith, et al., in: Crop Evapotranspiration-Guidelines For Computing Crop Water Requirements-Fao Irrigation and Drainage Paper 56, 300, FAO, Rome, 1998, p. D05109.
[19] M. de Carvalho Alves, L. Sanches, J. de Souza Nogueira, V.A.M. Silva, Effects of sky conditions measured by the clearness index on the estimation of solar radiation using a digital elevation model, Atmo-spheric Climate Sci. 2013 (2013).
[20] W. Smith, P. Wessel, Gridding with continuous curvature splines in tension, Geophysics 55 (3) (1990) 293–305.
[21] S. Khalil, A. Shaffie, Performance of statistical comparison models of solar energy on horizontal and inclined surface, Int. J. Energy Power 2 (1) (2013).
[22] M.A. Ahmed, S.A. Shaikh, Solar radiation studies for Dubai and Sharjah, UAE, World Acad. Sci., Eng. Technol. 73 (2013) 1007–1014.
[23] S. Tahas¸, D. Ristoiu, C. Cosma, Trends of the Global solar radiation and air temperature in Cluj-Napoca, Romania (1984-2008), Rom. J. Physiol. 56 (5/6) (2011) 784–789.
[24] A.K. Sunnu, Particle size and concentrations of the harmattan dust near the Gulf of Guinea, J. Environ. Sci. Eng. A 1 (10A) (2012) 1203.
[25] B. Tserenpurev, M. Shinoda, M. Tsubo, Effects of cloud, atmospheric water vapor, and dust on pho-tosynthetically active radiation and total solar radiation in a mongolian grassland, J. Arid Land 4 (4) (2012) 349–356.
[26] M. Mikami, G. Shi, I. Uno, S. Yabuki, Y. Iwasaka, M. Yasui, T. Aoki, T. Tanaka, Y. Kurosaki, K. Masuda, et al., Aeolian dust experiment on climate impact: an overview of Japan–China joint project adec, Global Planetary Change 52 (1) (2006) 142–172.
[27] M. Wild, D. Folini, C. Schar, N. Loeb, E.G. Dutton, G. Konig¨-Langlo, The global energy balance from a surface perspective, Climate Dyn. 40 (11–12) (2013) 3107–3134.